AIRR.SCIENCE · ARR-2026-4QVFJ65VWT9H5B8E v1 [Information theory] 28 Nov 2026

Quantum Entropic Metric Geometry: How Entanglement Reshapes Information Distance Cones

Lluis Eriksson*

November 28, 2026

Abstract

For an n-party quantum state $\rho_{A_0\cdots A_{n-1}}$, the *quantum variation of information*

$$d_Q(A_i, A_j) := S(A_i|A_j) + S(A_j|A_i) = 2S(A_iA_j) - S(A_i) - S(A_j)$$

measures the symmetric entanglement cost of bidirectional quantum state merging between subsystems A_i and A_j. Unlike its classical Shannon counterpart—which is automatically a semimetric on the polymatroid cone POLY_n—negative quantum conditional entropy allows d_Q to break the triangle inequality even when every pairwise conditional entropy $S(A_i|A_j)$ is nonnegative. Restricting to semimetric projections defines two nested hierarchies inside MET_n: the classical/polymatroid chain $\mathrm{CUT}_n \subseteq \mathrm{SUB}_n \subseteq \mathrm{VI}_n \subseteq \mathrm{POLY}_n$ and the quantum chain $\mathcal{M}_n^{\mathrm{cb},+} \subseteq \mathcal{M}_n^{\mathrm{q},+} \subseteq \mathcal{M}_n^{\mathrm{q}} \subseteq \mathcal{Q}_n := \Pi_n(\mathrm{QCONE}_n) \cap \mathrm{MET}_n$.

We establish the complete finite-party geometry and asymptotic obstruction theory of these cones through three main theorems, backed by exact rational certification and targeted zero-dependency Lean 4 kernel proofs. First, at $n \le 6$, we determine the exact phase hierarchy: $\mathrm{CUT}_n = \mathrm{MET}_n$ for $n \le 4$; $\mathrm{CUT}_5 \subsetneq \mathrm{SUB}_5 = \mathrm{MET}_5$ via $K_{2,3}$ over $\mathbb{F}_2^2$; and at $n = 6$,

$$\mathrm{CUT}_6 \subsetneq \mathrm{SUB}_6 \subseteq \mathrm{VI}_6 \subsetneq \mathrm{POLY}_6 \subsetneq \mathcal{M}_6^{\mathrm{cb},+} = \mathcal{M}_6^{\mathrm{q},+} = \mathrm{MET}_6,$$

proved by enumerating all 296 extreme rays of MET_6 (8 S_6-orbits, all realized in CB_6^+), all 1736 extreme rays of $\mathrm{POLY}_6 = \mathrm{MET}_6 \cap \{90 \text{ conjugates of } I_{K_{3,3}-e} \ge 0\}$ (12 orbits), and a Zhang–Yeung non-Shannon separation on Orbit 9 ($\kappa_{\mathrm{POLY}_6^{\mathrm{ZY}}} = 31/30$). Second, via the Segre quadric $Q^+(3, \mathbb{F}_q) \subset \mathbb{F}_q^{2\times 2}$, we prove a sharp bipartite dichotomy: $K_{m,m} \in \mathrm{SUB}_{2m}$ for every $m \ge 1$, whereas $K_{m,m} - e \notin \mathrm{POLY}_{2m}$ for every $m \ge 3$ ($\kappa_{\mathrm{POLY}_{2m}} \ge 9/8$). Across all 853 connected 7-vertex graphs, we isolate a transversal separation at Rem #4 (`G800`): it violates POLY_7 ($\kappa_{\mathrm{POLY}_7} = 17/16$) and CB_7 ($\kappa_{\mathrm{CB}_7} = \kappa_{\mathrm{CB}_7^+} = 13/12$, via an elementary 5-cycle inequality $F_4 \ge 0$), yet embeds isometrically in $\mathcal{M}_7^{\mathrm{q},+}$. Third, we discover two minimal universal quantum obstructions among the 853 graphs—QFail1 (`G708`, $\kappa_{\mathcal{Q}_7} = 21/20$) and QFail2 (`G873`, $\kappa_{\mathcal{Q}_7} = 41/40$)—forbidding isometric quantum realization in any Hilbert space of any dimension whenever present as an induced submetric. Finally, for the matching-deleted bipartite graphs $K_{m,m} - M$ ($n = 2m$), exact $\mathbb{Z}_2 \times S_m$ certification for $m = 3, \ldots, 18$ reveals an odd/even parity staircase: $\kappa_{\mathcal{Q}_{2m}}$ matches $\kappa_{\mathrm{POLY}_{2m}}$ at every even m yet drops strictly below at every odd $m \ge 5$, while for $m \le 18$, $\kappa_{\mathrm{POLY}_{2m}}$ matches the partial sums $1 + \sum_{k=3}^{\lfloor (m+1)/2 \rfloor} \frac{1}{2(k-1)!(k-1)(k-2)}$ of a factorial step series converging to $\frac{5-e}{2}$ (conjectured for all m).

*ORCID: 0009-0006-7494-9040; email: `editor@airr.science`. Manuscript licensed under CC-BY-4.0; verification code and Lean 4 proofs under MIT at https://github.com/lluiseriksson/quantum-entropic-metric-geometry (tag `v1.0.4`).

1 Introduction and Geometric Setup

Information distances turn probabilistic and algorithmic dependence into metric geometry. Given two random variables X_i, X_j with finite Shannon entropy, Rajski's variation of information [1]

$$d_H(X_i, X_j) := H(X_i|X_j) + H(X_j|X_i) = 2H(X_iX_j) - H(X_i) - H(X_j) \tag{1}$$

defines a canonical pseudometric whose Kolmogorov complexity analogue underpins the universal similarity distance of Bennett, Gács, Li, Vitányi, and Zurek [2], as well as modern metric formulations of algorithmic information distance by Hutter [9] and Hou [10]. Because Shannon entropy is monotone ($H(XY) \geq H(Y)$) and submodular ($H(XY)+H(YZ) \geq H(XYZ)+H(Y)$), every n-tuple of random variables—indeed, every polymatroid $h \in \Gamma_n$—automatically induces a semimetric $d_h \in \mathrm{MET}_n$. Classical information theory therefore sits comfortably *inside* the metric cone.

When random variables are replaced by subsystems $A_0, \ldots, A_{n-1}$ of an n-party quantum state $\rho_{A_0\cdots A_{n-1}}$ with von Neumann entropy $S(X) = -\operatorname{Tr}(\rho_X \log_2 \rho_X)$, the structural geometry changes fundamentally. Defining the *quantum variation of information* by the same formula,

$$d_Q(A_i, A_j) := S(A_i|A_j) + S(A_j|A_i) = 2S(A_iA_j) - S(A_i) - S(A_j), \tag{2}$$

gives d_Q a direct operational meaning: by the quantum state-merging protocol of Horodecki, Oppenheim, and Winter [6], $S(A_i|A_j)$ is the asymptotic entanglement rate required to merge A_i into A_j, so $d_Q(A_i, A_j)$ is the *bidirectional quantum state-merging cost* between parties i and j. Because entanglement makes $S(A_i|A_j)$ negative on a Bell pair $|\Phi^+\rangle_{ij}$ (where $S(i) = S(j) = 1$ and $S(ij) = 0$, giving $d_Q(i, j) = -2$), d_Q need not even be nonnegative on general states. Remarkably, even if we enforce pairwise nonnegativity $S(A_i|A_j) \geq 0$ everywhere—eliminating obvious negative distances—entanglement still breaks the triangle inequality.

Example 1.1 (Nonnegative pairwise conditional entropies do not imply a metric)**.** Consider the 4-party entropy vector given by the tensor average of two classical bits and two Bell pairs:

$$S_{\mathrm{CB}_4^+} := \tfrac{1}{4}\mathrm{cut}(\{0\}) + \tfrac{1}{4}\mathrm{cut}(\{2,3\}) + \tfrac{1}{4}|\Phi^+\rangle_{01} + \tfrac{1}{4}|\Phi^+\rangle_{12}, \tag{3}$$

where $\mathrm{cut}(T)$ distributes a single shared uniformly random classical bit to $T \subsetneq [n]$ and $|0\rangle$ to $[n] \setminus T$ (so $S_{\mathrm{cut}(T)}(X) = \mathbf{1}[X \cap T \neq \emptyset]$), and $|\Phi^+\rangle_{ab}$ contributes $S_{\Phi^+_{ab}}(X) = \mathbf{1}[|X \cap \{a, b\}| = 1]$. Explicitly, the 4-resource tensor-product state $\mathrm{cut}(\{0\}) \otimes \mathrm{cut}(\{2,3\}) \otimes |\Phi^+\rangle_{01} \otimes |\Phi^+\rangle_{12}$ realizes $4S_{\mathrm{CB}_4^+}$ directly as a quantum von Neumann entropy vector, placing (3) in $\mathrm{cone}(\Sigma_4^*)$ (and N-copy block normalization approaches (3) asymptotically in $\overline{\Sigma_4^*}$); alternatively, when an orthogonal classical mixture flag $p = (\frac{1}{4}, \frac{1}{4}, \frac{1}{4}, \frac{1}{4})$ is broadcast to every party $A_0, \ldots, A_{n-1}$, every nonempty subset entropy $S(X)$ shifts identically by $+H(p) = +2$, which cancels identically in both $S(i|j) = S(ij) - S(j)$ and $d_Q(i, j)$. For (3), direct calculation yields $4S(\{0\}) = 4S(\{1\}) = 4S(\{2\}) = 2$, $4S(\{3\}) = 1$, and pairwise joint entropies

$$\begin{aligned} &4S(\{0,1\}) = 2, \quad 4S(\{1,2\}) = 2, \quad 4S(\{0,2\}) = 4, \\ &4S(\{0,3\}) = 3, \quad 4S(\{1,3\}) = 3, \quad 4S(\{2,3\}) = 2. \end{aligned}$$

Thus $S(i|j) \geq 0$ for all 12 ordered pairs $i \neq j$ (with $\min_{i\neq j} S(i|j) = 0$), yet

$$d_Q(0,1) = 0, \qquad d_Q(1,2) = 0, \qquad d_Q(0,2) = 1,$$

violating $d_Q(0,2) \leq d_Q(0,1) + d_Q(1,2)$ (while $d_Q(0,3) = d_Q(1,3) = 3/4$ and $d_Q(2,3) = 1/4$).

Example 1.1 forces us to intersect entropic cones with the semimetric cone MET_n. Let $[n] := \{0, \dots, n-1\}$ and identify symmetric functions $d : \binom{[n]}{2} \to \mathbb{R}$ with vectors in $\mathbb{R}^{\binom{n}{2}}$.

Definition 1.2 (Entropic Metric Cones)**.** Let $\mathrm{MET}_n \subset \mathbb{R}^{\binom{n}{2}}$ be the closed polyhedral cone of semimetrics ($d_{ij} \geq 0$ and $d_{ij} + d_{jk} \geq d_{ik}$ for all distinct i, j, k). Define the linear projection $\Pi_n : \mathbb{R}^{2^n-1} \to \mathbb{R}^{\binom{n}{2}}$ by $(\Pi_n S)_{ij} := 2S(\{i,j\}) - S(\{i\}) - S(\{j\})$ (with $S(\emptyset) = 0$). Inside MET_n, we study two nested families of closed convex cones:

(a) *Classical and polymatroid cones:* $\mathrm{CUT}_n \subseteq \mathrm{SUB}_n \subseteq \mathrm{VI}_n \subseteq \mathrm{POLY}_n \subseteq \mathrm{MET}_n$, where:

- CUT_n is the conic hull of the $2^{n-1} - 1$ cut semimetrics $\delta_T(i,j) := \mathbf{1}[|T \cap \{i,j\}| = 1]$ ($\emptyset \neq T \subsetneq [n]$), with Deza–Laurent [12] providing the polyhedral foundations of CUT_n and MET_n;
- SUB_n is the closed conic hull of $\Pi_n(S)$ arising from linear subspace rank functions $S(X) = \dim_{\mathbb{F}_q}(\sum_{i \in X} V_i)$ over finite fields $\mathbb{F}_q$;
- $\mathrm{VI}_n := \overline{\Pi_n(\Gamma_n^*)}$ is the closure in $\mathbb{R}^{\binom{n}{2}}$ of all classical Shannon variation-of-information metrics;
- $\mathrm{POLY}_n := \Pi_n(\Gamma_n)$, where $\Gamma_n \subset \mathbb{R}^{2^n-1}$ is the Shannon polymatroid cone defined by monotonicity ($h([n]) \geq h([n] \setminus \{i\})$) and elemental submodularity ($h(iK) + h(jK) \geq h(ijK) + h(K)$).

(b) *Quantum and entanglement cones:* $\mathcal{M}_n^{\mathrm{cb},+} \subseteq \mathcal{M}_n^{\mathrm{q},+} \subseteq \mathcal{M}_n^{\mathrm{q}} \subseteq \mathcal{Q}_n$, where:

- $\mathrm{CB}_n := \mathrm{cone}\{\mathrm{cut}(T) : \emptyset \neq T \subsetneq [n]\} + \mathrm{cone}\{|\Phi^+\rangle_{ij} : 0 \leq i < j < n\}$ in entropy space, $\mathrm{CB}_n^+ := \{S \in \mathrm{CB}_n : S(i|j) \geq 0 \ \forall i \neq j\}$, $\mathcal{M}_n^{\mathrm{cb}} := \Pi_n(\mathrm{CB}_n) \cap \mathrm{MET}_n$, and $\mathcal{M}_n^{\mathrm{cb},+} := \Pi_n(\mathrm{CB}_n^+) \cap \mathrm{MET}_n$;
- $\mathcal{M}_n^{\mathrm{q}} := \overline{\Pi_n(\Sigma_n^*)} \cap \mathrm{MET}_n$ is the closure of all quantum d_Q semimetrics, and $\mathcal{M}_n^{\mathrm{q},+} := \overline{\Pi_n(\Sigma_n^{*,+})} \cap \mathrm{MET}_n$, where $\Sigma_n^{*,+} := \{S \in \Sigma_n^* : S(i|j) \geq 0 \ \forall i \neq j\}$;
- $\mathcal{Q}_n := \Pi_n(\mathrm{QCONE}_n) \cap \mathrm{MET}_n$, where QCONE_n is Pippenger's basic quantum entropy cone [5] cut out by Lieb–Ruskai strong subadditivity (SSA) [11] and weak monotonicity (WM).

For the polyhedral cones $\mathrm{POLY}_n = \Pi_n(\Gamma_n)$, $\mathcal{Q}_n = \Pi_n(\mathrm{QCONE}_n) \cap \mathrm{MET}_n$, $\mathcal{M}_n^{\mathrm{cb}}$, and $\mathcal{M}_n^{\mathrm{cb},+}$, linear projections are automatically closed by the Minkowski–Weyl theorem; by contrast, the classical and quantum entropic regions Γ_n^* and Σ_n^* have non-polyhedral closures $\overline{\Gamma_n^*}$ and $\overline{\Sigma_n^*}$ (which are convex cones meeting $\ker(\Pi_n)$ nontrivially along $\mathbb{R}_{\geq 0}\mathbf{1}$ and S_{GHZ_n}), so closure is taken directly in metric space $\mathbb{R}^{\binom{n}{2}}$. Notice also that because $\Pi_n(\Sigma_n^{*,+}) \subseteq \Pi_n(\Sigma_n^*)$ contains the interior point $\mathbf{1} \in \mathrm{int}(\mathrm{MET}_n)$ (realized by n independent fair classical bits) and the closures of quantum entropy projections are convex cones, $\overline{\Pi_n(\Sigma_n^*) \cap \mathrm{MET}_n} = \overline{\Pi_n(\Sigma_n^*)} \cap \mathrm{MET}_n$ (and likewise for $\mathcal{M}_n^{\mathrm{q},+}$), so $\mathcal{M}_n^{\mathrm{q}}$ coincides with the closure of all quantum d_Q semimetrics. For any cone $\mathcal{C} \subseteq \mathrm{MET}_n$ and nonzero $d \in \mathrm{MET}_n$, the *optimal multiplicative metric distortion* of d into $\mathcal{C}$ is

$$\kappa_{\mathcal{C}}(d) := \inf\{\kappa \geq 1 : \exists\, d' \in \mathcal{C} \text{ such that } d_{ij} \leq d'_{ij} \leq \kappa\, d_{ij} \ \forall\, i < j\}.$$

For entropy cones $\mathcal{E} \in \{\mathrm{CB}_n, \mathrm{CB}_n^+\}$, we likewise write $\kappa_{\mathcal{E}}(d) := \kappa_{\Pi_n(\mathcal{E})}(d)$ for distortion into the unrestricted projection $\Pi_n(\mathcal{E})$; on all 853 connected 7-vertex graphs, direct LP verification shows $\kappa_{\mathrm{CB}_7}(G) = \kappa_{\mathcal{M}_7^{\mathrm{cb}}}(G)$ identically (and $\kappa_{\mathrm{CB}_7^+}(\text{Rem \#4}) = \kappa_{\mathcal{M}_7^{\mathrm{cb},+}}(\text{Rem \#4}) = 13/12$).

Throughout this paper we adhere to a maximal-strength asymmetry: every *achievability* or realization theorem is proved inside the strongest pairwise-nonnegative cones ($\mathcal{M}_n^{\mathrm{cb},+}$ or $\mathcal{M}_n^{\mathrm{q},+}$), whereas every *impossibility* or distortion lower bound is proved against the weakest outer cones

(POLY_n, $\mathcal{M}_n^{\mathrm{cb}}$, or $\mathcal{Q}_n$). Notice also that every cut and every Bell pair satisfies SSA and WM, so $\mathcal{M}_n^{\mathrm{cb},+} \subseteq \mathcal{M}_n^{\mathrm{cb}} \subseteq \mathcal{Q}_n$; similarly, $\mathrm{POLY}_n \subseteq \mathcal{Q}_n$ because monotonicity plus submodularity implies both SSA and WM. Moreover, because every classical Shannon entropy vector $h \in \Gamma_n^*$ satisfies monotonicity $H(X_i|X_j) \geq 0$, we have $\Pi_n(\Gamma_n^*) \subseteq \Pi_n(\Sigma_n^{*,+}) \cap \mathrm{MET}_n$, so $\mathrm{CUT}_n \subseteq \mathrm{SUB}_n \subseteq \mathrm{VI}_n \subseteq \mathcal{M}_n^{\mathrm{q},+}$ holds unconditionally.

Before analyzing specific dimensions, we record a clean 4-line characterization of QCONE_n that eliminates all redundant inequalities in our exact linear programs and Lean 4 proofs.

Proposition 1.3 (Purification Reduction of QCONE_n)**.** *For every $n \geq 2$, QCONE_n is cut out by exactly $\binom{n}{2}2^{n-2} + n \cdot 2^{n-2}$ elemental inequalities:*

$$S(iK) + S(jK) - S(ijK) - S(K) \geq 0 \qquad (i < j,\ K \subseteq [n] \setminus \{i,j\}), \tag{4}$$

$$S(iK) + S(iL) - S(K) - S(L) \geq 0 \qquad (i \in [n],\ K \sqcup L = [n] \setminus \{i\},\ K < L). \tag{5}$$

Proof. Introduce a purifying system E and extend S on $[n]$ to S^* on $[n] \cup \{E\}$ via $S^*(X) = S(X)$ and $S^*(X \cup \{E\}) = S([n] \setminus X)$ for $X \subseteq [n]$ (with $S^*(\emptyset) = S^*([n] \cup \{E\}) = 0$). Any general weak monotonicity inequality $S(AB) + S(BC) \geq S(A) + S(C)$ on pairwise disjoint $A, B, C \subseteq [n]$ with $D := [n] \setminus (ABC)$ rewrites identically as general SSA on $(B, A, D \cup \{E\})$ in $[n] \cup \{E\}$:

$$S^*(BA) + S^*(A(D \cup \{E\})) - S^*(BA(D \cup \{E\})) - S^*(A) = S(AB) + S(BC) - S(C) - S(A).$$

Telescoping general SSA on $[n] \cup \{E\}$ into elemental SSA inequalities on $[n] \cup \{E\}$ and substituting $S^*(X \cup \{E\}) = S([n] \setminus X)$ sends every instance with $E \notin \{x, y\} \cup K$ or $E \in K$ to (4), and every instance with $E \in \{x, y\}$ to (5). General subadditivity $S(A) + S(B) \geq S(AB)$ $(A \cap B = \emptyset)$ follows by telescoping (4) over $i \in A, j \in B$; applying subadditivity to the purified extension $S^*(X) + S^*(([n] \cup \{E\}) \setminus X) \geq S^*([n] \cup \{E\}) = 0$ then gives $2S(X) \geq 0$, so nonnegativity uses both (4) and (5). □

2 Theorem 1: Exact $n \leq 6$ Phase Hierarchy and Entanglement Metric Universality

Classical and quantum entropic metrics are indistinguishable for $n \leq 4$, diverge classically from cuts at $n = 5$, and explode into a five-stage separation at $n = 6$—where, remarkably, classical bits plus Bell pairs under $S(i|j) \geq 0$ recover the *entire* metric cone MET_6.

Theorem 2.1 (Exact $n \leq 6$ Phase Hierarchy)**.** *The entropic metric cones satisfy:*

(1) For $n \leq 4$, all classical and quantum cones collapse to MET_n: MET_3 has 3 extreme rays (1 orbit) and MET_4 has 7 extreme rays (2 orbits), all cut metrics [12].

(2) For $n = 5$, $\mathrm{CUT}_5 \subsetneq \mathrm{SUB}_5 = \mathrm{VI}_5 = \mathrm{POLY}_5 = \mathcal{M}_5^{\mathrm{cb},+} = \mathcal{M}_5^{\mathrm{q},+} = \mathrm{MET}_5$. Specifically, MET_5 has 25 extreme rays in 3 S_5-orbits [12]: 15 cuts (sizes $5 + 10$) and 10 copies of the bipartite metric $K_{2,3}$, which is realized in SUB_5 over $\mathbb{F}_2^2$.

(3) For $n = 6$, we have the strict phase hierarchy

$$\mathrm{CUT}_6 \subsetneq \mathrm{SUB}_6 \subseteq \mathrm{VI}_6 \subsetneq \mathrm{POLY}_6 \subsetneq \mathcal{M}_6^{\mathrm{cb},+} = \mathcal{M}_6^{\mathrm{q},+} = \mathrm{MET}_6. \tag{6}$$

More precisely:

(i) MET_6 *has exactly* 296 *extreme rays forming* 8 S_6*-orbits of sizes* $(6, 15, 10, 60, 90, 15, 10, 90)$ *[12]. Orbits* 1–7 *lie in* SUB_6*, Orbit* 8 *is* $K_{3,3} - e$*, and all* 8 *orbits (*296 *rays) lie in* CB_6^+*, proving* $\mathcal{M}_6^{\mathrm{cb},+} = \mathcal{M}_6^{\mathrm{q},+} = \mathrm{MET}_6$*.*

(ii) On POLY_6*,* $K_{3,3} - e$ *(with bipartition* $A = \{0, 1, 2\}, B = \{3, 4, 5\}$ *and missing edge* $(2, 5)$*) satisfies the facet inequality*

$$I_{K_{3,3}-e}(d) := 2 \sum_{e \in E(K_{3,3}-e)} d(e) - \sum_{p \in \binom{A}{2} \cup \binom{B}{2}} d(p) - 2\, d(2, 5) \geq 0,$$

certified by an exact integer 10*-orbit* D_4*-symmetrized Shannon Farkas identity, with exact optimal distortion* $\kappa_{\mathrm{POLY}_6}(K_{3,3} - e) = 9/8$*.*

(iii) Intersecting MET_6 *with the* 90 S_6*-conjugates of* $I_{K_{3,3}-e}(d) \geq 0$ *yields a pointed cone with exactly* 1736 *extreme rays in* 12 S_6*-orbits of sizes* $(6, 15, 10, 60, 90, 15, 10, 90, 360, 360, 360, 360)$*. Every one of the* 12 *orbits admits an exact rational polymatroid in* Γ_6*, proving* $\mathrm{POLY}_6 = \mathrm{MET}_6 \cap \{90$ *conjugates of* $I_{K_{3,3}-e} \geq 0\}$*.*

(iv) Let $\mathrm{POLY}_6^{\mathrm{ZY}} := \Pi_6(\Gamma_6 \cap \mathrm{ZY}_6)$ *denote the projection of* Γ_6 *intersected with all* 1680 S_6*-permuted Zhang–Yeung non-Shannon inequalities [3]. Orbit* 9 *(size* 360*) separates* VI_6 *from* POLY_6 *with exact distortion* $\kappa_{\mathrm{POLY}_6^{\mathrm{ZY}}}(\mathit{Orbit}\ 9) = 31/30$*, while Orbits* 1–8 *and* 10–12 *satisfy all* 1680 *Zhang–Yeung inequalities (*$\kappa_{\mathrm{POLY}_6^{\mathrm{ZY}}} = 1$*). Moreover, Orbit* 9 *admits an explicit* 6*-atom realization in* CB_6^+*.*

(v) Among all 112 *connected* 6*-vertex graphs,* 110 *embed isometrically into* POLY_6*, and exactly* 2 *fail* POLY_6*:* $K_{3,3} - e$ *(*`G154`*,* $\kappa_{\mathrm{POLY}_6} = 9/8$*) and* `G168` *(*$\kappa_{\mathrm{POLY}_6} = 17/16$*); both embed isometrically into* $\mathcal{M}_6^{\mathrm{cb},+}$*.*

Proof. We establish each stage via exact rational polyhedral geometry and explicit algebraic witnesses.

Stage $n \leq 5$**.** Exact GMP Double Description (`cdd.gmp`) of the defining inequalities of MET_n yields 3 cut rays (1 orbit) for $n = 3$, 7 cut rays (2 orbits of sizes $4, 3$) for $n = 4$, and 25 extreme rays (3 orbits of sizes $5, 10, 10$) for $n = 5$. The sole non-cut orbit at $n = 5$ is the shortest-path metric of $K_{2,3}$ with parts $\{0, 4\}$ and $\{1, 2, 3\}$. Assigning party 0 the zero subspace $\{0\} \leq \mathbb{F}_2^2$, party 4 the full space $\mathbb{F}_2^2$, and parties $1, 2, 3$ the three distinct 1-dimensional lines $\langle(1, 0)\rangle, \langle(0, 1)\rangle, \langle(1, 1)\rangle \leq \mathbb{F}_2^2$ gives $d(0, 4) = 2(2) - 0 - 2 = 2$, $d(0, i) = 2(1) - 0 - 1 = 1$, $d(4, i) = 2(2) - 2 - 1 = 1$, and $d(i, j) = 2(2) - 1 - 1 = 2$ for $1 \leq i < j \leq 3$, proving $K_{2,3} \in \mathrm{SUB}_5$. Because $\mathrm{CUT}_5 \subsetneq \mathrm{SUB}_5 \subseteq \mathrm{VI}_5 \subseteq \mathrm{POLY}_5 \subseteq \mathrm{MET}_5$ and $\mathrm{SUB}_5 \subseteq \mathrm{VI}_5 \subseteq \mathcal{M}_5^{\mathrm{q},+} \subseteq \mathcal{M}_5^{\mathrm{q}} \subseteq \mathcal{Q}_5 \subseteq \mathrm{MET}_5$, this immediately collapses $\mathrm{SUB}_5 = \mathrm{VI}_5 = \mathrm{POLY}_5 = \mathcal{M}_5^{\mathrm{q},+} = \mathcal{M}_5^{\mathrm{q}} = \mathcal{Q}_5 = \mathrm{MET}_5$. To prove that $\mathcal{M}_5^{\mathrm{cb},+}$ also equals MET_5, we directly exhibit an explicit 5-atom witness in CB_5^+ for $K_{2,3}$ on $\{0, 4\} \sqcup \{1, 2, 3\}$:

$$S_{K_{2,3}}^{\mathrm{CB}_5^+} := \tfrac{1}{2}\mathrm{cut}(\{3\}) + \tfrac{1}{2}\mathrm{cut}(\{0, 1, 3, 4\}) + \mathrm{cut}(\{2, 3, 4\}) + \tfrac{1}{2}(|\Phi^+\rangle_{02} + |\Phi^+\rangle_{03}),$$

whose singletons are $(\frac{3}{2}, \frac{1}{2}, \frac{3}{2}, \frac{5}{2}, \frac{3}{2})$ with $\min_{i \neq j} S(i|j) = 0 \geq 0$ and all 10 pairwise distances equal to $d_{K_{2,3}}$, proving $K_{2,3} \in \mathcal{M}_5^{\mathrm{cb},+}$ and hence $\mathcal{M}_5^{\mathrm{cb},+} = \mathcal{M}_5^{\mathrm{q},+} = \mathrm{MET}_5$.

Stage $n = 6$**:** MET_6 **extreme rays and** $\mathrm{SUB}_6 \cup \mathcal{M}_6^{\mathrm{cb},+}$**.** Exact GMP Double Description of MET_6 yields 296 primitive integer extreme rays partitioned into 8 S_6-orbits (Table 1). Orbits 1–3 are the 31 classical cut metrics. Orbits 4 and 5 collapse one vertex pair ($d_{01} = 0$) onto the $K_{2,3}$ realization over $\mathbb{F}_2^2$. Orbit 6 is $K_{2,4}$, realized over $\mathbb{F}_3^2$ by assigning party 0 to $\{0\}$, party 5 to $\mathbb{F}_3^2$, and parties

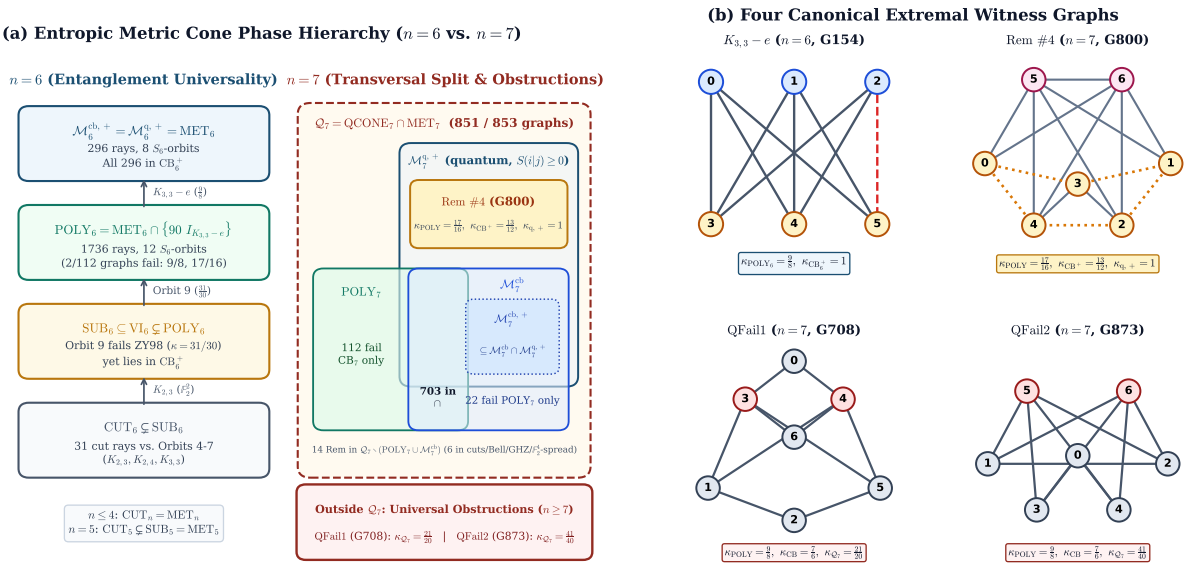

Figure 1: The entropic metric cone phase hierarchy at $n = 6$ and $n = 7$ (panel a) and the four canonical extremal witness graphs (panel b) separating POLY_6 from $\mathcal{M}_6^{\mathrm{cb},+}$, establishing Rem #4 $\in \mathcal{M}_7^{\mathrm{q},+} \setminus (\mathrm{POLY}_7 \cup \mathcal{M}_7^{\mathrm{cb}})$ inside $\mathcal{Q}_7$, and separating QFail1, QFail2 from the outer quantum cone $\mathcal{Q}_7$.

$1, 2, 3, 4$ to the four lines of $\mathbb{P}^1(\mathbb{F}_3)$ ($\langle(1,0)\rangle, \langle(0,1)\rangle, \langle(1,1)\rangle, \langle(1,2)\rangle$). Orbit 7 is $K_{3,3}$, realized over $\mathbb{F}_2^4$ by the Segre quadric $Q^+(3, \mathbb{F}_2)$ (proved in general in Section 3). Hence Orbits 1–7 all lie in SUB_6.

Remarkably, solving the exact rational cone-membership linear program over the 62 classical cuts and 15 Bell pairs subject to $S(i|j) \geq 0$ (30 constraints) succeeds with $\kappa = 1$ on all 8 orbits—including Orbit 8 ($K_{3,3} - e$), which with bipartition $A = \{0, 1, 2\}, B = \{3, 4, 5\}$ and missing edge $(2, 5)$ is realized cleanly in CB_6^+ by

$$\tfrac{1}{2}\mathrm{cut}(\{2\}) + \tfrac{1}{2}\mathrm{cut}(\{0,1,2,3,4\}) + \mathrm{cut}(\{0,3,5\}) + \tfrac{1}{2}\big(|\Phi^+\rangle_{13} + |\Phi^+\rangle_{15} + |\Phi^+\rangle_{23}\big).$$

Since CB_6^+ is S_6-invariant and convex, all 296 extreme rays of MET_6 lie in $\mathcal{M}_6^{\mathrm{cb},+}$, establishing $\mathcal{M}_6^{\mathrm{cb},+} = \mathcal{M}_6^{\mathrm{q},+} = \mathrm{MET}_6$.

The D_4-symmetrized Farkas certificate for $I_{K_{3,3}-e} \geq 0$. Relabeling Row 8 to $A = \{0, 1, 2\}$, $B = \{3, 4, 5\}$, and missing edge $(2, 5)$, the automorphism group $\mathrm{Aut}(K_{3,3} - e) \cong D_4$ of order 8 is generated by $(0\,1)$, $(3\,4)$, and the bipartition swap $(0\,3)(1\,4)(2\,5)$. Partitioning the 246 elemental Shannon inequalities of Γ_6 into D_4-orbits yields 54 orbits; Table 2 exhibits an exact positive integer combination of 10 D_4-orbits whose summed left-hand side equals $\Pi_6^T c_{K_{3,3}-e}$ identically on all 63 nonempty subsets of $[6]$, where $c_{K_{3,3}-e}$ assigns $+2$ to each of the 8 edges, -1 to each of the 6 same-side pairs, and -2 to $(2, 5)$. Thus $I_{K_{3,3}-e}(d) \geq 0$ holds on all of POLY_6. On $d_{K_{3,3}-e}$, the positive terms sum to $2 \cdot 8 = 16$ while the negative terms sum to $6 \cdot 2 + 2 \cdot 3 = 18$, forcing $\kappa_{\mathrm{POLY}_6}(K_{3,3} - e) \geq 18/16 = 9/8$ (also kernel-certified in Lean 4, Theorem `k33e_poly6_distortion_ge_9_8`). Conversely, define the explicit D_4-symmetric function $h : 2^{[6]} \to \mathbb{Q}_{\geq 0}$ ($h(\emptyset) = 0$, $p := |X \cap A|$, $q := |X \cap B|$) by $h(X) := 3$ if $\{2, 5\} \subseteq X$, and for $\{2, 5\} \not\subseteq X$ by $h(X) := 3/2$ if $|X| = 1$; $33/16$ if $(p, q) = (1, 1)$; $5/2$ if $\{p, q\} = \{2, 0\}$; $21/8$ if $\{p, q\} = \{2, 1\}$;

Table 1: Complete S_6-orbit classification of the 296 extreme rays of MET_6 and the 4 additional new orbits of $\mathrm{POLY}_6 = \mathrm{MET}_6 \cap \{90 \text{ conjugates of } I_{K_{3,3}-e} \geq 0\}$ (1736 total rays). Row 8's canonical representative has bipartition $\{0,4,5\} \sqcup \{1,2,3\}$ with missing edge $(3,5)$.

Orbit	Size	Representative d (pairs $01, 02, \ldots, 45$)	Geometric Type	$\in \mathrm{SUB}_6$?	κ_{POLY_6}	$\kappa_{\mathrm{POLY}_6^{\mathrm{ZY}}}$
1	6	$(0,0,0,0,1,0,0,0,1,0,0,1,0,1,1)$	Cut (1+5)	Yes ($\mathbb{F}_2$)	1	1
2	15	$(0,0,0,1,1,0,0,1,1,0,1,1,1,1,0)$	Cut (2+4)	Yes ($\mathbb{F}_2$)	1	1
3	10	$(0,0,1,1,1,0,1,1,1,1,1,1,0,0,0)$	Cut (3+3)	Yes ($\mathbb{F}_2$)	1	1
4	60	$(0,1,1,1,2,1,1,1,2,2,2,1,2,1,1)$	Collapsed $K_{2,3}$	Yes ($\mathbb{F}_2^2$)	1	1
5	90	$(0,1,1,2,2,1,1,2,2,2,1,1,1,1,2)$	Collapsed $K_{2,3}$	Yes ($\mathbb{F}_2^2$)	1	1
6	15	$(1,1,1,1,2,2,2,2,1,2,2,1,2,1,1)$	$K_{2,4}$ ($\mathbb{P}^1(\mathbb{F}_3)$)	Yes ($\mathbb{F}_3^2$)	1	1
7	10	$(1,1,1,2,2,2,2,1,1,2,1,1,1,1,2)$	$K_{3,3}$ ($Q^+(3,\mathbb{F}_2)$)	Yes ($\mathbb{F}_2^4$)	1	1
8 (MET_6)	**90**	$(1,1,1,2,2,2,2,1,1,2,1,1,1,3,2)$	$K_{3,3} - e$	No	**9/8**	–
8 (POLY_6)	90	$(1,1,1,2,2,2,2,1,1,2,1,1,1,2,2)$	Truncated $K_{3,3} - e$	–	1	1
9 (POLY_6)	**360**	$(1,1,2,3,3,2,3,2,2,3,2,4,1,1,2)$	**ZY98-violating ray**	No	1	**31/30**
10 (POLY_6)	360	$(1,2,2,4,4,3,3,3,5,4,2,2,2,2,4)$	Facet ray	–	1	1
11 (POLY_6)	360	$(2,2,3,4,5,4,5,2,3,5,6,3,3,2,5)$	Facet ray	–	1	1
12 (POLY_6)	360	$(3,3,3,4,6,6,6,3,3,6,3,3,7,3,6)$	Facet ray	–	1	1

Table 2: Exact integer 10-orbit D_4-symmetrized Shannon Farkas proof of $I_{K_{3,3}-e}(d) \geq 0$ on POLY_6 (where $I(i:j \mid K) = h(iK) + h(jK) - h(ijK) - h(K) \geq 0$).

Orbit	Mult.	Weight y	Representative Inequality	Orbit	Mult.	Weight y	Representative Inequality
0	8	2	$I(0:2 \mid \{3\}) \geq 0$	36	4	1	$I(0:2 \mid \{1,3,4,5\}) \geq 0$
8	2	2	$I(0:1 \mid \{3,4\}) \geq 0$	43	4	1	$I(0:3 \mid \{2,5\}) \geq 0$
17	4	2	$I(0:1 \mid \{3,5\}) \geq 0$	44	4	2	$I(0:1 \mid \{2,3,5\}) \geq 0$
26	4	1	$I(0:2 \mid \{1,3,4\}) \geq 0$	47	4	3	$I(0:3 \mid \{1,2,4,5\}) \geq 0$
27	4	1	$I(2:5 \mid \{0,1,3\}) \geq 0$	48	4	4	$h([6]) - h([6] \setminus \{0\}) \geq 0$

11/4 if $(p,q) = (2,2)$; and 23/8 when $\max(p,q) = 3$. Verifying all 246 elemental inequalities (6 monotonicity and 240 submodularity, checked in `code/verify_quantum_entropic_metrics.py`) confirms $h \in \Gamma_6$, while $\Pi_6(h)$ assigns 9/8 to every edge of $K_{3,3} - e$, 2 to every same-side pair, and 3 to $(2,5)$, satisfying $d_{K_{3,3}-e} \leq \Pi_6(h) \leq \frac{9}{8} d_{K_{3,3}-e}$ and proving $\kappa_{\mathrm{POLY}_6}(K_{3,3} - e) = 9/8$.

Exact Double Description of POLY_6 and Orbit 9 non-Shannon separation. Using exact integer Fukuda–Prodon Double Description starting from the 296 rays of MET_6 and intersecting sequentially with the 90 S_6-conjugates of $I_{K_{3,3}-e}(d) \geq 0$, we obtain 1736 primitive integer rays in 12 S_6-orbits (Table 1), each verified independently to satisfy all 150 inequalities and achieve tight-constraint rank $14 = \dim \mathrm{MET}_6 - 1$. Solving the exact rational LP $h \in \Gamma_6, \Pi_6(h) = d$ for each of the 12 orbit representatives succeeds with $\kappa = 1$, proving $\mathrm{POLY}_6 = \mathrm{MET}_6 \cap \{90\}$.

Testing all 12 orbit representatives against the 1680 S_6-permuted Zhang–Yeung inequalities [3],

$$2I(C:D) \leq I(A:B) + I(A:CD) + 3I(C:D|A) + I(C:D|B),$$

over all disjoint nonempty $A, B, C, D \subset [6]$, Orbits 1–8 and 10–12 achieve $\kappa = 1$, whereas **Orbit** 9 fails with exact distortion $\kappa_{\mathrm{POLY}_6^{\mathrm{ZY}}}(\text{Orbit } 9) = 31/30$: dual weights 1/60 on the two Zhang–Yeung instances $(A,B,C,D) = (\{2\},\{5\},\{1\},\{4\})$ and $(\{5\},\{2\},\{1\},\{4\})$ combined with 32 elemental Shannon terms satisfy $\alpha \cdot d_{\mathrm{Orb9}} = 31/30$ and $\beta \cdot d_{\mathrm{Orb9}} = 1$ (clearing denominators yields an integer inequality $c_9 \cdot d \geq 0$ evaluating to -4 on Orbit 9). Since $\mathrm{VI}_6 \subseteq \mathrm{POLY}_6^{\mathrm{ZY}}$, this strictly separates $\mathrm{VI}_6 \subsetneq \mathrm{POLY}_6$. Meanwhile, Orbit 9 lies in CB_6^+ via the explicit 6-atom entropy vector in CB_6^+

$$2\,\mathrm{cut}(\{0,1,2\}) + \tfrac{1}{2}\mathrm{cut}(\{5\}) + \tfrac{1}{2}\mathrm{cut}(\{0,1,3,4,5\}) + \tfrac{1}{2}|\Phi^+\rangle_{14} + \tfrac{1}{2}|\Phi^+\rangle_{15} + \tfrac{1}{2}|\Phi^+\rangle_{24}.$$

Finally, checking all 112 connected 6-vertex graphs in exact rational arithmetic confirms that 110 embed isometrically into POLY_6 while only `G154` ($K_{3,3} - e$, $\kappa_{\mathrm{POLY}_6} = 9/8$) and `G168` (edges $\{(0,2),(0,3),(0,5),(1,2),(1,3),(2,3),(2,4),(3,4),(4,5)\}$, $\kappa_{\mathrm{POLY}_6} = 17/16$) fail; both lie in $\mathcal{M}_6^{\mathrm{cb},+}$. □

3 Theorem 2: Hyperbolic-Quadric Dichotomy and $n = 7$ Transversal Separation

At $n = 7$, the inclusion $\mathrm{POLY}_6 \subsetneq \mathcal{M}_6^{\mathrm{cb},+}$ shatters into genuine transversal incomparability: classical polymatroids and classical-plus-Bell entanglement separate in opposite directions, while full bipartite entanglement with linear subspace atoms contains both on our benchmark witness.

Theorem 3.1 (Hyperbolic-Quadric Dichotomy and $n = 7$ Separation)**.**

(1) ***Segre Quadric Dichotomy:*** *For every prime power q and every $1 \le m \le q+1$, the two opposite reguli of the hyperbolic quadric $Q^+(3,\mathbb{F}_q) \subset \mathbb{F}_q^{2\times 2}$ realize the complete bipartite metric $K_{m,m} \in \mathrm{SUB}_{2m} \subseteq \mathrm{VI}_{2m}$; because arbitrarily large prime powers q exist, $K_{m,m} \in \mathrm{SUB}_{2m}$ holds for every $m \ge 1$. By contrast, for every $m \ge 3$, deleting a single edge breaks polymatroid realizability: $K_{m,m} - e \notin \mathrm{POLY}_{2m}$, with $\kappa_{\mathrm{POLY}_{2m}}(K_{m,m} - e) \ge 9/8$.*

(2) ***Exhaustive*** *$n = 7$* ***Graph Partition:*** *Across all* 853 *connected* 7*-vertex graphs,* 38 *fail* POLY_7*,* 128 *fail* CB_7*,* 16 *fail both* POLY_7 *and* CB_7*, and exactly* 2 *(*QFail1 = `G708`*,* QFail2 = `G873`*) fail $\mathcal{Q}_7$, leaving* 703 *in* $\mathrm{POLY}_7 \cap \mathcal{M}_7^{\mathrm{cb}}$*,* 112 *in* $\mathrm{POLY}_7 \setminus \mathcal{M}_7^{\mathrm{cb}}$*,* 22 *in* $\mathcal{M}_7^{\mathrm{cb}} \setminus \mathrm{POLY}_7$*, and* 14 *in* $\mathcal{Q}_7 \setminus (\mathrm{POLY}_7 \cup \mathcal{M}_7^{\mathrm{cb}})$*.*

(3) ***Bipartite-vs-Subspace Separation at*** Rem #4***:*** *The* 7*-vertex graph* Rem #4 *(`G800`, index* 4 *of the* 14 *remaining graphs, edge set* $\{(0,5),(0,6),(1,5),(1,6),(2,3),(2,5),(2,6),(3,4),(4,5),(4,6),(5,6)\}$*) satisfies:*

- *(i)* Rem #4 $\notin \mathrm{POLY}_7$*, with exact Farkas-certified distortion* $\kappa_{\mathrm{POLY}_7}(\text{Rem \#4}) = 17/16$*;*
- *(ii)* Rem #4 $\notin \mathcal{M}_7^{\mathrm{cb}}$ *(even without $S(i|j) \ge 0$), certified by the elementary* 5*-cycle inequality*

$$F_4(d) := \sum_{x\in\{0,1,2,3,4\}} (d(x,5) + d(x,6)) - d(5,6) - \sum_{e\in C_5} d(e) \ge 0 \tag{7}$$

  where $C_5 = \{(0,3),(3,1),(1,2),(2,4),(4,0)\}$, satisfying $\min_{cuts} F_4 = 0$ over all 126 *cuts, $\min_{Bell} F_4 = 0$ over all* 21 *Bell pairs, $F_4(d_{\mathrm{Rem\#4}}) = -1$, and exact distortions $\kappa_{\mathrm{CB}_7} = \kappa_{\mathrm{CB}_7^+} = 13/12$ on* Rem #4*;*

- *(iii)* Rem #4 $\in \mathcal{M}_7^{\mathrm{q},+}$ *isometrically ($\kappa = 1$), realized by an explicit binary-qubit state combining $|\Phi^+\rangle_{34}$, a private bit, an $\mathbb{F}_2^2$ atom, and an $\mathbb{F}_2^4$-spread $K_{2,4}$ subspace atom with $\min_{i\ne j} S(i|j) = 0 \ge 0$.*

Consequently, POLY_7 *and* $\mathcal{M}_7^{\mathrm{cb}}$ *(as well as* $\mathcal{M}_7^{\mathrm{cb},+}$*) are incomparable, and* $\mathcal{M}_7^{\mathrm{q},+} \not\subseteq \mathrm{POLY}_7 \cup \mathcal{M}_7^{\mathrm{cb}}$ *(witnessed by* Rem #4 $\in \mathcal{M}_7^{\mathrm{q},+} \setminus (\mathrm{POLY}_7 \cup \mathcal{M}_7^{\mathrm{cb}})$*).*

Proof. **Part (1): Segre Quadric $Q^+(3,\mathbb{F}_q)$.** Identify $\mathbb{F}_q^4$ with the space $\mathbb{F}_q^{2\times 2}$ of 2×2 matrices over $\mathbb{F}_q$. For each projective point $u = [u_0 : u_1] \in \mathbb{P}^1(\mathbb{F}_q)$ ($q+1$ points in total), define the 2-dimensional left-regulus and right-regulus subspaces

$$L_u := \{xu^T : x \in \mathbb{F}_q^2\}, \qquad M_v := \{vy^T : y \in \mathbb{F}_q^2\}.$$

If $u \neq u'$ in $\mathbb{P}^1(\mathbb{F}_q)$, any matrix $A \in L_u \cap L_{u'}$ has row space contained in $\mathrm{span}(u) \cap \mathrm{span}(u') = \{0\}$, so $L_u \cap L_{u'} = \{0\}$ and $\dim(L_u + L_{u'}) = 4$ (verified algebraically over an arbitrary field in Lean 4, `segre_same_regulus_disjoint`). Likewise $M_v \cap M_{v'} = \{0\}$ for $v \neq v'$. Conversely, for any pair $(u, v) \in \mathbb{P}^1(\mathbb{F}_q)^2$, every matrix $A \in L_u \cap M_v$ has row space in $\mathrm{span}(u)$ and column space in $\mathrm{span}(v)$, so $L_u \cap M_v = \mathrm{span}(vu^T)$ is exactly 1-dimensional (`segre_opp_regulus_rank_one`), giving $\dim(L_u + M_v) = 2 + 2 - 1 = 3$. Measuring entropy in units of $2\log_2 q$ (dividing rank by 2), the $2(q+1)$ subspaces $\{L_u\}, \{M_v\}$ yield

$$d(L_u, L_{u'}) = d(M_v, M_{v'}) = \tfrac{1}{2}(2 \cdot 4 - 2 - 2) = 2, \qquad d(L_u, M_v) = \tfrac{1}{2}(2 \cdot 3 - 2 - 2) = 1,$$

realizing $K_{q+1,q+1} \in \mathrm{SUB}_{2q+2}$, and restricting to $m \leq q+1$ points per regulus gives $K_{m,m} \in \mathrm{SUB}_{2m}$. For the fracture converse ($m \geq 3$), any missing edge $e = (a, b)$ in $K_{m,m} - e$ lies inside an induced $3 + 3$ subgraph on $A' \sqcup B'$ containing $a \in A', b \in B'$. Because $K_{m,m} - e$ has diameter 3 and $d(u, v) = 1, d(u, u') = 2, d(a, b) = 3$ on $A' \sqcup B'$, this 6-vertex restriction is isometric to $K_{3,3} - e$, so Theorem 2.1 gives $\kappa_{\mathrm{POLY}_{2m}}(K_{m,m} - e) \geq 9/8$.

Part (2): Exhaustive $n = 7$ graph classification. Using exact rational linear programming (`DomainMatrix` over $\mathbb{Q}$) across all 853 connected 7-vertex graphs in the Graph Atlas confirms the exact counts $(38, 128, 16, 2)$ in POLY_7, CB_7, $\mathrm{POLY}_7 \cap \mathrm{CB}_7$ failures, and $\mathcal{Q}_7$ failures, respectively (Figure 2a).

Part (3): Proof of Rem #4 **separation.** Exact Farkas dual certification yields $\kappa_{\mathrm{POLY}_7}(\text{Rem \#4}) = 17/16$ (with a 44-term Shannon proof). To prove Rem #4 $\notin \mathrm{CB}_7$, evaluate F_4 from (7) directly:

- *All* 126 *classical cuts* δ_T*:* If $5, 6$ lie on the same side of the cut ($d(5, 6) = 0$), then for each $x \in \{0, \ldots, 4\}$, $d(x, 5) + d(x, 6) = 2\,\mathbf{1}[x \text{ separated from } \{5, 6\}]$, while each separated vertex in C_5 contributes at most 2 cut edges of C_5, so $F_4(\delta_T) \geq 0$. If $5, 6$ lie on opposite sides ($d(5, 6) = 1$), then $d(x, 5) + d(x, 6) = 1$ for all five x, giving $\sum_x (d(x, 5) + d(x, 6)) = 5$; meanwhile an odd 5-cycle C_5 can have at most 4 cut edges, so $F_4(\delta_T) \geq 5 - 1 - 4 = 0$.
- *All* 21 *Bell pairs* $|\Phi^+\rangle_{ab}$*:* Recall $d_{\Phi^+_{ab}}(i, j) = -2$ for $\{i, j\} = \{a, b\}$, $+1$ if $|\{i, j\} \cap \{a, b\}| = 1$, and 0 otherwise. Checking the four $S_2 \times D_5$ orbits of $\{a, b\}$: for $\{5, 6\}$, $F_4 = 10 - (-2) - 0 = 12$; for $\{a, b\}$ with $a \in \{5, 6\}, b \in C_5$, $F_4 = (-1+4) - 1 - 2 = 0$; for $ab \in E(C_5)$, $F_4 = 4 - 0 - (-2+2) = 4$; and for non-adjacent $a, b \in C_5$, $F_4 = 4 - 0 - 4 = 0$.

Both exhaustive checks are also kernel-verified over all 128 bitmasks and 21 pairs in Lean 4 (`F4_nonneg_on_all_128_cuts`, `F4_nonneg_on_all_21_bells`). On $d_{\mathrm{Rem\#4}}$, vertices $0, 1, 2, 4$ are adjacent to $\{5, 6\}$ while vertex 3 sits at distance 2 from $\{5, 6\}$; on C_5, $(2, 3)$ and $(3, 4)$ are edges, $(0, 4), (1, 2), (2, 4)$ have distance 2, and $(0, 3), (1, 3)$ have distance 3, while $(5, 6)$ is an edge. Thus

$$F_4(d_{\mathrm{Rem\#4}}) = (8 \cdot 1 + 2 \cdot 2) - \big(1 + (3 + 3 + 2 + 2 + 2)\big) = 12 - 13 = -1,$$

forcing $\kappa_{\mathrm{CB}_7}(\text{Rem \#4}) \geq 13/12$, which is matched by an explicit CB_7^+ primal realization ($\kappa_{\mathrm{CB}_7} = \kappa_{\mathrm{CB}_7^+} = 13/12$).

Finally, to realize Rem #4 isometrically in $\mathcal{M}_7^{\mathrm{q},+}$, recall that $\mathbb{F}_2^4 \cong \mathbb{F}_4^2$ admits a 2-spread of five mutually disjoint 2-planes $W_0, W_1, W_2, W_3, W_4 \leq \mathbb{F}_2^4$ (the five points of $\mathbb{P}^1(\mathbb{F}_4)$, satisfying $W_a \cap W_b = \{0\}$ and $W_a + W_b = \mathbb{F}_2^4$ for $a \neq b$). Define the 4-atom binary-qubit / classical-subspace state

$$S_{\mathrm{Rem\#4}}(X) := \tfrac{1}{4}\Big(2S_{|\Phi^+\rangle_{34}}(X) + 2S_{\mathrm{bit}(3)}(X) + 2S_{\mathbb{F}_2^2}(X) + S_{\mathbb{F}_2^4}(X)\Big), \tag{8}$$

where:

- $S_{\mathbb{F}_2^2}$ assigns $(0,1,2,3) \mapsto (\langle e_1\rangle, \langle e_2\rangle, \langle e_1+e_2\rangle, \langle e_1+e_2\rangle)$ and $(4,5,6) \mapsto \{0\}$ in $\mathbb{F}_2^2$;
- $S_{\mathbb{F}_2^4}$ assigns $(0,1,2,3,4,5,6) \mapsto (W_0, W_1, W_2, W_2, W_4, \mathbb{F}_2^4, \{0\})$ in $\mathbb{F}_2^4$ (a $K_{2,4}$-spread atom with $2,3$ glued to W_2).

Clearing the factor $1/4$ realizes $4S_{\text{Rem\#4}}$ by an exact finite tensor product of two Bell pairs on $(3,4)$, two private classical bits at party 3, two copies of $\mathbb{F}_2^2$, and one copy of $\mathbb{F}_2^4$. Checking all 21 pairs reproduces $d_{\text{Rem\#4}}$ identically (with singletons $S(i) = (1,1,1,2,1,1,0)$ and total entropy $S([7]) = 5/2$), and every ordered pair $i \neq j$ satisfies $S(i|j) \geq 0$ (minimum 0), proving Rem $\#4 \in \mathcal{M}_7^{\mathrm{q},+}$. □

4 Theorem 3: Universal Quantum Obstructions and the $K_{m,m} - M$ Parity Staircase

While $\mathcal{M}_7^{\mathrm{q},+}$ absorbs Rem #4 and all but 2 of the 853 connected 7-vertex graphs, those remaining 2 graphs break even the outer quantum cone $\mathcal{Q}_7$—and thereby induce universal obstructions across all $n \geq 7$. Pushing further to bipartite graphs with a removed matching $K_{m,m} - M$ exposes an unexpected parity oscillation between polymatroids and quantum states.

Theorem 4.1 (Universal Obstructions and the $K_{m,m} - M$ Parity Staircase)**.**

(1) ***Universal Quantum Impossibility*** *($n \geq 7$): Among all* 853 *connected* 7*-vertex graphs, exactly two fail $\mathcal{Q}_7$:*

- QFail1 *(`G708`), edges* $\{(0,3),(0,4),(1,2),(1,3),(1,4),(2,5),(3,5),(3,6),(4,5),(4,6)\}$*, with exact Farkas-certified distortion* $\kappa_{\mathcal{Q}_7}(\text{QFail1}) = 21/20$ *(and* $\kappa_{\text{POLY}_7} = 9/8$*,* $\kappa_{\text{CB}_7} = 7/6$*);*
- QFail2 *(`G873`), edges* $\{(0,3),(0,4),(1,2),(1,5),(1,6),(2,5),(2,6),(3,5),(3,6),(4,5),(4,6)\}$*, with exact Farkas-certified distortion* $\kappa_{\mathcal{Q}_7}(\text{QFail2}) = 41/40$ *(and* $\kappa_{\text{POLY}_7} = 9/8$*,* $\kappa_{\text{CB}_7} = 7/6$*).*

By isometric restriction, no metric space (X,d) of any cardinality $n \geq 7$ containing an isometric copy of QFail1 *or* QFail2 *can be realized by any quantum state in any Hilbert space.*

(2) ***The $K_{m,m} - M$ Matching Barrier*** *($m = 5, n = 10$): On $K_{5,5} - M$, an exact* 15*-orbit $\mathbb{Z}_2 \times S_5$ SSA+WM identity certifies the valid quantum metric inequality (per-pair weights* $(11, -8, -3)$*)*

$$11 \sum_{r \neq s} d(a_r, b_s) - 8 \sum_{r=0}^{4} d(a_r, b_r) - 3 \sum_{\{u,u'\} \in \binom{A}{2} \cup \binom{B}{2}} d(u,u') \geq 0 \qquad (\text{on } \mathcal{Q}_{10}), \tag{9}$$

yielding the strict triple separation

$$\frac{12}{11} = \kappa_{\mathcal{Q}_{10}}(K_{5,5} - M) \;<\; \frac{9}{8} = \kappa_{\text{POLY}_{10}}(K_{5,5} - M) \;<\; \frac{4}{3} = \kappa_{\text{CUT}_{10}}(K_{5,5} - M).$$

(3) ***Exact Odd/Even Parity Staircase*** *($m = 3, \ldots, 18$): For all $m = 3, \ldots, 18$ ($n = 2m$), exact rational $\mathbb{Z}_2 \times S_m$ primal and dual certification gives the values in Table 5. In particular:*

- *For every* even $m \in \{4, 6, \ldots, 18\}$*,* $\kappa_{\mathcal{Q}_{2m}}(K_{m,m} - M) = \kappa_{\text{POLY}_{2m}}(K_{m,m} - M)$*.*
- *For every* odd $m \in \{5, 7, \ldots, 17\}$*,* $\kappa_{\mathcal{Q}_{2m}}(K_{m,m} - M) < \kappa_{\text{POLY}_{2m}}(K_{m,m} - M)$*.*

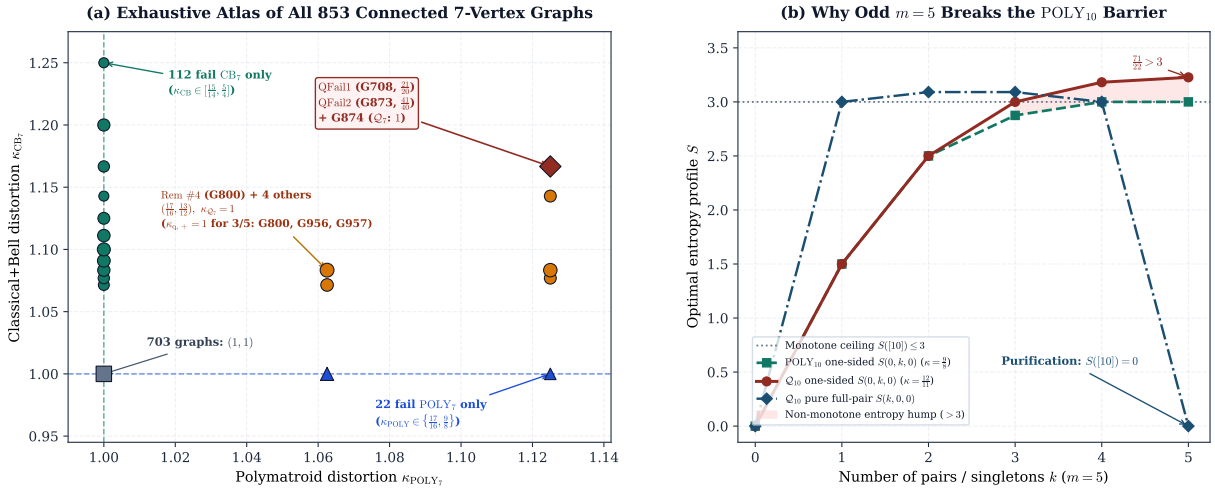

Figure 2: (a) Complete distortion atlas of all 853 connected 7-vertex graphs in $(\kappa_{\mathrm{POLY}_7}, \kappa_{\mathrm{CB}_7})$ coordinates. (b) Comparison of the optimal entropy profiles along one bipartition side $S(0,k,0)$ and full-pair subsets $S(k,0,0)$ at $m=5$ $(n=10)$: omitting monotonicity allows $\mathcal{Q}_{10}$ to form a pure-state entropy hump exceeding 3 before purifying to $S([10])=0$, dropping $\kappa_{\mathcal{Q}_{10}} = 12/11$ below $\kappa_{\mathrm{POLY}_{10}} = 9/8$.

- *Across all* $m = 3, \ldots, 18$, $\kappa_{\mathrm{POLY}_{2m}}(K_{m,m} - M)$ *obeys the exact factorial step series*

$$\kappa_{\mathrm{POLY}_{2m}}(K_{m,m} - M) = 1 + \sum_{k=3}^{\lfloor (m+1)/2 \rfloor} \frac{1}{2(k-1)!(k-1)(k-2)}, \tag{10}$$

  whose infinite limit evaluates in closed form to $\frac{5-e}{2} \approx 1.14085908577$.

Proof. **Part (1): Isometric restriction and** QFail1**,** QFail2**.** If $\iota : [k] \hookrightarrow [n]$ is an isometric embedding of (Y, d_Y) into (X, d), any metric $d' \in \mathcal{Q}_n$ with $d \le d' \le \kappa d$ lifts to an abstract entropy vector $S \in \mathrm{QCONE}_n$ with $\Pi_n(S) = d'$. By definition, QCONE_n is cut out by strong subadditivity and all weak monotonicity inequalities $S(A) + S(B) \ge S(A \setminus B) + S(B \setminus A)$ $(A, B \subseteq [n])$, which by Proposition 1.3 are equivalent to (4)–(5). Restricting S to subsets of $\iota([k])$ retains the sub-family of SSA and WM inequalities supported on $\iota([k])$, so $S|_{\iota([k])} \in \mathrm{QCONE}_k$ (verified formally in Lean 4, `isometric_restriction_preserves_qcone`) and $\Pi_k(S|_{\iota([k])}) = d'|_{\iota([k])}$. Thus $\kappa_{\mathcal{Q}_k}(d_Y) \le \kappa_{\mathcal{Q}_n}(d)$.

For QFail1 (`G708`), exact basis inversion produces a 36-term integer Farkas identity (30 elemental SSA and 6 elemental WM inequalities) proving $\alpha \cdot d_{\mathrm{G708}} = 42$ and $\beta \cdot d_{\mathrm{G708}} = 40$, so $\kappa_{\mathcal{Q}_7}(\mathrm{QFail1}) \ge 42/40 = 21/20$ (kernel-certified in Lean 4, `qfail1_q7_distortion_ge_21_20`). Conversely, the left half of Table 3 lists an explicit $\mathrm{Aut}(\mathrm{G708})$-symmetric pure-state rational primal $S_1 \in \mathrm{QCONE}_7$ $(40\, S_1(X) \in \mathbb{Z},\ S_1([7]) = 0,\ S_1(X) = S_1([7] \setminus X))$ verified in `code/verify_quantum_entropic_metrics.py` against all 896 elemental SSA+WM inequalities (672 SSA + 224 WM from Proposition 1.3) and achieving $d_{\mathrm{G708}} \le \Pi_7(S_1) \le \frac{21}{20} d_{\mathrm{G708}}$ (e.g., $d_Q(0,3) = (2 \cdot 95 - 67 - 81)/40 = 21/20$), proving $\kappa_{\mathcal{Q}_7}(\mathrm{QFail1}) = 21/20$.

For QFail2 (`G873`), its $\mathbb{Z}_2^3$ automorphism group $(1 \leftrightarrow 2,\ 3 \leftrightarrow 4,\ 5 \leftrightarrow 6)$ yields a completely symmetric 46-term integer Farkas identity (36 SSA and 10 WM terms) certifying the $\mathcal{Q}_7$-valid

Table 3: Explicit matching pure-state $\mathrm{Aut}(G)$-symmetric rational primals in QCONE_7 for QFail1 (`G708`, left, $40\,S_1(X) \in \mathbb{Z}$, $\kappa \le 21/20$) and QFail2 (`G873`, right, $80\,S_2(X) \in \mathbb{Z}$, $\kappa \le 41/40$) across all 26 complementary orbit pairs ($S([7]) = 0$, $S(X) = S([7] \setminus X)$). Both satisfy all 896 elemental SSA+WM inequalities of Proposition 1.3.

QFail1 (`G708`)			QFail2 (`G873`)		
Rep. X	Mult.	$40\,S_1(X)$	Rep. X	Mult.	$80\,S_2(X)$
$\{0\}$	4	67	$\{0\}$	2	98
$\{1\}$	4	81	$\{1\}$	4	142
$\{0,1\}$	8	114	$\{0,1\}$	4	240
$\{2\}$	2	53	$\{1,2\}$	2	182
$\{0,2\}$	4	120	$\{0,1,2\}$	2	240
$\{1,2\}$	4	88	$\{3\}$	4	166
$\{0,1,2\}$	8	118	$\{0,3\}$	4	173
$\{3\}$	4	81	$\{1,3\}$	8	234
$\{0,3\}$	8	95	$\{0,1,3\}$	8	238
$\{1,3\}$	8	102	$\{1,2,3\}$	4	234
$\{0,1,3\}$	16	116	$\{3,5,6\}$	4	238
$\{2,3\}$	4	109	$\{3,4\}$	2	246
$\{0,2,3\}$	8	123	$\{0,3,4\}$	2	236
$\{1,2,3\}$	8	109	$\{1,3,4\}$	4	246
$\{3,4\}$	2	121	$\{1,5,6\}$	4	236
$\{0,3,4\}$	4	116	$\{0,5,6\}$	2	246
$\{1,3,4\}$	4	123	$\{5,6\}$	2	236
$\{2,3,4\}$	2	131	$\{5\}$	4	156
$\{0,1,5\}$	4	126	$\{0,5\}$	4	209
$\{0,1,6\}$	4	130	$\{1,5\}$	8	190
$\{1,5\}$	2	121	$\{0,1,5\}$	8	243
$\{1,2,5\}$	2	111	$\{1,2,5\}$	4	209
$\{1,3,5\}$	4	123	$\{3,4,5\}$	4	243
$\{0,3,6\}$	4	109	$\{3,5\}$	8	202
$\{0,2,6\}$	2	125	$\{0,3,5\}$	8	209
$\{0,6\}$	2	107	$\{1,3,5\}$	16	236

inequality

$$5\sum_{u\in\{3,4\}}\big(d(u,5)+d(u,6)\big)+3\sum_{v\in\{1,2\}}\big(d(v,5)+d(v,6)\big)+2\big(d(0,3)+d(0,4)\big)+d(0,5)+d(0,6)$$
$$-5\,d(5,6)-2\,d(3,4)-d(1,2)-3\big(d(0,1)+d(0,2)\big)-\sum_{\substack{v\in\{1,2\}\\u\in\{3,4\}}}d(v,u)\ge 0.$$

On d_{G873}, the positive terms evaluate to 40 and the negative terms evaluate to 41, giving $\kappa_{\mathcal{Q}_7}(\mathrm{QFail2}) \ge 41/40$ (kernel-certified in Lean 4, `qfail2_q7_distortion_ge_41_40`). Conversely, the right half of Table 3 gives an explicit $\mathbb{Z}_2^3$-symmetric pure-state rational primal $S_2 \in \mathrm{QCONE}_7$ ($80\,S_2(X) \in \mathbb{Z}$, $S_2([7]) = 0$, $S_2(X) = S_2([7] \setminus X)$) satisfying all 896 elemental SSA+WM inequalities (672 SSA + 224 WM) and $d_{\mathrm{G873}} \le \Pi_7(S_2) \le \frac{41}{40} d_{\mathrm{G873}}$ (for example, $d_Q(0,3) = (2{\cdot}173{-}98{-}166)/80 = 41/40$ and $d_Q(1,2) = (2\cdot 182 - 142 - 142)/80 = 1$), completing the proof that $\kappa_{\mathcal{Q}_7}(\mathrm{QFail2}) = 41/40$.

Part (2): Symmetry reduction and the $m = 5$ certificate. Let $K_{m,m} - M$ have bipartition $A = \{a_0, \dots, a_{m-1}\}$, $B = \{b_0, \dots, b_{m-1}\}$, and missing matching $M = \{(a_r, b_r)\}_{r=0}^{m-1}$. Its automorphism group $G = \mathbb{Z}_2 \times S_m$ acts by diagonal permutations of indices $r \in [m]$ and the swap $A \leftrightarrow B$. Every subset $X \subseteq A \sqcup B$ is classified up to G by counts (k_{11}, k_{10}, k_{01}) of pairs r where $|X \cap \{a_r, b_r\}|$

Table 4: Exact integer 15-orbit $\mathbb{Z}_2 \times S_5$ SSA+WM Farkas proof of (9) at $m = 5$ ($n = 10$), certifying $11\, d_{\text{edge}} - 3\, d_{\text{same}} - 2\, d_{\text{match}} \geq 0$ and $\kappa_{\mathcal{Q}_{10}}(K_{5,5} - M) = 12/11$. Weights $11y$ rescale the dual multipliers y solving $\sum_{\mathcal{O}} y_{\mathcal{O}} M_{\mathcal{O}} = \Pi^T(\beta - \alpha)$ (with $\beta_{\text{edge}} = 1$, $\alpha_{\text{same}} = 3/11$, $\alpha_{\text{match}} = 2/11$). Signature 3-tuples (k_{11}, k_{10}, k_{01}) count $(1,1)$, $(1,0)$, and $(0,1)$ background pairs on the remaining $m-1$ matching edges (SSA-match, WM, with the active party's removed matching mate placed in L rather than K for WM); 5-tuples $(u, v, k_{11}, k_{10}, k_{01})$ record mate-inclusion bits $u, v \in \{0,1\}$ for the active pair followed by the background signature on the remaining $m-2$ pairs (SSA-same, SSA-edge).

Weight ($11y$)	Inequality Orbit	Signature	Weight ($11y$)	Inequality Orbit	Signature
2	SSA-match	$(0,0,1)$	4	WM	$(1,0,0)$
10	SSA-same	$(0,0,0,0,1)$	2	SSA-same	$(0,0,1,1,0)$
2	SSA-match	$(0,0,2)$	2	SSA-same	$(0,0,1,2,0)$
6	SSA-same	$(0,0,0,0,2)$	2	SSA-match	$(1,0,2)$
2	SSA-match	$(0,1,2)$	4	SSA-same	$(1,1,1,0,1)$
2	SSA-same	$(0,0,0,1,2)$	2	SSA-match	$(1,0,3)$
2	WM	$(2,2,0)$	4	SSA-same	$(1,1,2,0,0)$
2	SSA-edge	$(0,1,0,0,3)$	Orbit $\Pi^T(\beta-\alpha)$: $11d_{\text{edge}} - 3d_{\text{same}} - 2d_{\text{match}} \geq 0$		

has signature $(1,1)$, $(1,0)$, or $(0,1)$, canonicalized under $k_{10} \leftrightarrow k_{01}$ to $k_{10} \geq k_{01}$ with $k_{11} + k_{10} + k_{01} \leq m$. By convexity and G-invariance of QCONE_{2m} and POLY_{2m}, a G-symmetric metric $(d_{\text{edge}}, d_{\text{same}}, d_{\text{match}})$ (here $(1,2,3)$) is realized within distortion κ if and only if a G-invariant entropy vector $S(k_{11}, k_{10}, k_{01})$ achieves it under all G-orbits of elemental SSA (3 matching-pair types), WM, and monotonicity.

At $m = 5$, Table 4 gives the exact 15-orbit integer Farkas certificate on the 33-variable reduced system proving $11d_{\text{edge}} - 3d_{\text{same}} - 2d_{\text{match}} \geq 0$ on $\mathcal{Q}_{10}$ (kernel-certified in Lean 4, Theorem `k55m_q10_distortion_ge_12_11`). Distributing the orbit weights uniformly across the 20 edges, 20 same-side pairs, and 5 matching pairs and clearing 20 yields (9). Evaluating (9) on $(1,2,3)$ gives $11 \cdot 20 \cdot 1 = 220$ versus $8 \cdot 5 \cdot 3 + 3 \cdot 20 \cdot 2 = 240$, proving $\kappa_{\mathcal{Q}_{10}} \geq 240/220 = 12/11$ (matched by an exact rational primal in Table 5). Solving the same symmetry-reduced system for POLY_{10} and CUT_{10} yields $\kappa_{\text{POLY}_{10}} = 9/8$ and $\kappa_{\text{CUT}_{10}} = 4/3$.

Part (3): The Parity Staircase and $(5-e)/2$ series. Exact rational primal and dual solutions for $m = 3, \ldots, 18$ appear in Table 5 and Figure 3. Geometrically, the odd/even split reflects how Weak Monotonicity interacts with purification complementarity across the bipartition (Figure 2b). Under POLY_{2m}, monotonicity locks every subset entropy below the global cap $S([2m]) = 3$ (for instance, the minimal-entropy primal satisfies $S_{\text{POLY}}(0,k,0) = (0, \frac{3}{2}, \frac{5}{2}, \frac{23}{8}, 3, 3)$ at $m = 5$ and $(0, \frac{3}{2}, \frac{5}{2}, \frac{23}{8}, 3, 3, 3)$ at $m = 6$). Under $\mathcal{Q}_{2m}$, the optimal pure-state solution obeys $S(X) = S(X^c)$ and $S([2m]) = 0$, permitting $S(X)$ to rise above 3 at mid-size subsets before returning to 0. When $m = 2k$ is *even*, A and B bisect symmetrically into halves of size k, enabling complementary midpoint WM constraints (specifically $\text{WM}(0,0,3)$ paired with $\text{WM}(1,1,0)$ in the exact $m = 6$ dual) to clamp the one-sided profile $S(0,j,0)$ onto the monotone polymatroid ceiling. When $m = 2k-1$ is *odd*, no equal integer bisection of A exists, leaving a parity slack of 1 party that allows a non-monotone entropy hump exceeding 3 (e.g., $S_{\mathcal{Q}_{10}}(A) = 71/22 > 3$ at $m = 5$), lowering $\kappa_{\mathcal{Q}_{2m}}$ strictly below $\kappa_{\text{POLY}_{2m}}$.

Finally, verifying (10) for $m = 3, \ldots, 18$ is immediate from Table 5, where successive increments for $k = 3, \ldots, 9$ are $1/8$, $1/72$, $1/576$, $1/4800$, $1/43200$, $1/423360$, and $1/4515840$. To evaluate the

Table 5: Exact rational $\mathbb{Z}_2 \times S_m$-certified distortions of $K_{m,m} - M$ for $m = 3, \ldots, 18$ ($n = 2m$).

m	n	$\kappa_{\mathrm{CUT}_{2m}}$	$\kappa_{\mathrm{POLY}_{2m}}$	$\kappa_{\mathcal{Q}_{2m}}$	Parity Gap $\kappa_{\mathrm{POLY}} - \kappa_{\mathcal{Q}}$
3	6	1	1	1	0
4	8	1	1	1	0
5	10	4/3	9/8	12/11	3/88
6	12	4/3	9/8	9/8	0
7	14	3/2	41/36	25/22	1/396
8	16	3/2	41/36	41/36	0
9	18	8/5	73/64	65/57	1/3648
10	20	8/5	73/64	73/64	0
11	22	5/3	1369/1200	397/348	1/34800
12	24	5/3	1369/1200	1369/1200	0
13	26	–	9857/8640	1871/1640	1/354240
14	28	–	9857/8640	9857/8640	0
15	30	–	26833/23520	22589/19800	1/3880800
16	32	–	26833/23520	26833/23520	0
17	34	–	735991/645120	81649/71568	1/45803520
18	36	–	735991/645120	735991/645120	0

infinite series in closed form, note that for $j = k - 1 \geq 2$,

$$\sum_{j=2}^{\infty} \frac{1}{j!\, j(j-1)} = \sum_{j=2}^{\infty} \left(\frac{1}{j!(j-1)} - \frac{1}{j!\, j} \right) = \int_0^1 \frac{(1-t)(e^t - 1 - t)}{t^2}\, dt.$$

Using the exact derivative identity

$$\frac{d}{dt}\left(\frac{1 + t - e^t}{t} \right) = \frac{(1-t)(e^t - 1 - t)}{t^2} - 1,$$

integrating over $t \in [0, 1]$ yields $\sum_{j=2}^{\infty} \frac{1}{j!j(j-1)} = 1 + (2 - e) - 0 = 3 - e$. Halving and adding 1 gives the exact transcendental limit $1 + \frac{3-e}{2} = \frac{5-e}{2} \approx 1.14085908577$. □

5 Formal and Exact Rational Verification

All numerical classifications and exact rational certificates in Theorems 2.1–4.1 are verified deterministically over $\mathbb{Q}$ in Python, while the 39 theorems mechanized in zero-dependency Lean 4.36.0 independently machine-check the core algebraic, structural, and Farkas-kernel identities (including Proposition 1.3, isometric restriction, and the principal distortion lower bounds), hosted at `https://github.com/lluiseriksson/quantum-entropic-metric-geometry` (tag `v1.0.4`):

1. **Exact Rational Python Verifier** (`code/verify_quantum_entropic_metrics.py`, `tests/test_verification.py`): uses `scipy.optimize.linprog` solely to locate candidate supports and then performs all polyhedral enumerations (`cdd.gmp` and exact Fukuda–Prodon Double Description), linear system inversions (sparse `DomainMatrix` over $\mathbb{Q}$), primal feasibility checks, and Farkas dual identity verifications strictly in exact integer and `fractions.Fraction` arithmetic. All 4 module-level test suites in `pytest` pass cleanly, covering all 296 rays of MET_6, all 1736 rays of POLY_6 (with exact rank-14 tightness verification), all 112 connected 6-vertex graphs, all 853 connected 7-vertex graphs, and the full $m = 3 \ldots 18$ parity staircase.

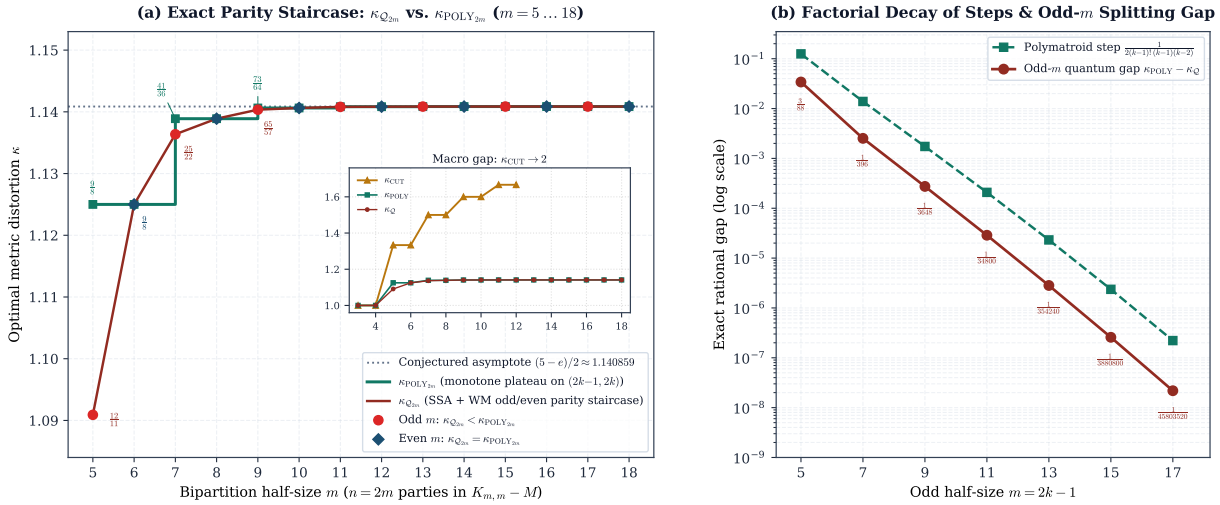

Figure 3: (a) The $K_{m,m} - M$ distortion staircase ($m = 5 \ldots 18$): $\kappa_{\mathrm{POLY}_{2m}}$ steps at odd m and plateaus on $(2k-1, 2k)$, while $\kappa_{\mathcal{Q}_{2m}}$ locks onto $\kappa_{\mathrm{POLY}_{2m}}$ at every even m and drops strictly below at every odd m, both consistent with convergence toward $(5-e)/2$ (Open Problem 6.2). Inset: macro gap against $\kappa_{\mathrm{CUT}_{2m}} \to 2$. (b) Factorial decay of the step increments and the odd-m quantum parity gap on a logarithmic scale.

2. **Targeted Lean 4.36.0 Kernel Mechanization** (`lean/QuantumEntropicMetrics.lean`): compiles with `lean -DwarningAsError=true` with 0 errors, 0 warnings, 0 imports, 0 `sorry`, 0 `native_decide`, and 0 `Classical.choice` axioms (verified via `#print axioms`). It proves: (i) the general integer Conic Farkas Distortion Theorem (`farkas_distortion_bound`); (ii) purification duality (`purification_ssa_gives_wm`); (iii) isometric restriction validity for QCONE_n (`isometric_restriction_preserves_qcone`); (iv) the CB_4^+ triangle violation under $S(i|j) \geq 0$; (v) the Segre quadric $Q^+(3, \mathbb{F})$ incidence and rank-one intersection identities over an arbitrary field (`segre_same_regulus_disjoint`, `segre_opp_regulus_rank_one`); (vi) $F_4 \geq 0$ across all 128 classical cuts and 21 Bell pairs together with $F_4(d_{\mathrm{Rem}\#4}) = -1$; and (vii) unconditional kernel-verified distortion bounds for $K_{3,3} - e$ (9/8), QFail1 (21/20), QFail2 (41/40), and $K_{5,5} - M$ at $m = 5$ (12/11).

Attribution and Verification Scope. Classical variation-of-information metrics trace to Rajski [1], polyhedral cut and metric cones to Deza and Laurent [12], algorithmic information distance to Bennett et al. [2], Hutter [9], and Hou [10], non-Shannon polymatroid facets to Zhang and Yeung [3], strong subadditivity of von Neumann entropy to Lieb and Ruskai [11], quantum entropy cones to Pippenger [5] and Linden–Winter [7], and quantum state merging to Horodecki, Oppenheim, and Winter [6]. Our exact rational certifications hold unconditionally for $n \leq 7$ and $m \leq 18$; the persistence of (10) for $m \geq 19$ is stated below as an open problem rather than a proved theorem. Parts of the computational exploration, exact certificate extraction, and Lean 4 proof engineering were carried out with Google Antigravity AI assistance under author supervision and independent exact-rational and kernel verification.

6 Open Problems

Open Problem 6.1 (Sep #0 and Multipartite vs. Subspace+Bell Realizability). In our classification of the 14 graphs in $\mathcal{Q}_7 \setminus (\mathrm{POLY}_7 \cup \mathcal{M}_7^{\mathrm{cb}})$, 6 graphs (including Rem #4 = `G800`) are already realized by Bell pairs plus $\mathbb{F}_2^4$-spread subspace atoms, whereas the remaining 8—starting with Sep #0 (`G550`, edge set $\{(0,1),(0,5),(0,6),(1,2),(1,4),(2,3),(2,5),(3,4),(4,5)\}$, $\kappa_{\mathrm{POLY}_7} = 9/8$, $\kappa_{\mathrm{CB}_7} = 8/7$, $\kappa_{\mathcal{Q}_7} = 1$)—defy all mixtures of classical cuts, Bell pairs, GHZ states, and $\mathbb{F}_2^4$-spread atoms. Does Sep #0 embed isometrically into $\mathcal{M}_7^{\mathrm{q},+}$ via non-stabilizer or higher-rank multipartite entangled states, or is it separated from $\mathcal{M}_7^{\mathrm{q},+}$ by constrained quantum entropy inequalities beyond SSA+WM (such as Cadney–Linden–Winter [8] or holographic inequalities)?

Open Problem 6.2 (Analytic Proof of the $(5-e)/2$ Staircase Limit). Establish analytically for all $m \geq 3$ that $\kappa_{\mathrm{POLY}_{2m}}(K_{m,m} - M)$ equals the partial sum (10) and that $\kappa_{\mathcal{Q}_{2m}}(K_{m,m} - M) = \kappa_{\mathrm{POLY}_{2m}}(K_{m,m} - M)$ for every even $m = 2k$. Together with the isometric sandwich $\kappa_{\mathrm{POLY}_{4k-4}} \leq \kappa_{\mathcal{Q}_{4k-2}} \leq \kappa_{\mathrm{POLY}_{4k-2}}$ for $k \geq 3$, this would rigorously prove

$$\lim_{m\to\infty} \kappa_{\mathcal{Q}_{2m}}(K_{m,m} - M) = \lim_{m\to\infty} \kappa_{\mathrm{POLY}_{2m}}(K_{m,m} - M) = \frac{5-e}{2}.$$

Open Problem 6.3 (Bourgain's Expander Barrier in $\mathcal{Q}_n$). By Bourgain's theorem and the Linial–London–Rabinovich bound [4], any n-vertex constant-degree expander graph G incurs classical ℓ_1/cut distortion $\kappa_{\mathrm{CUT}_n}(G) = \Omega(\log n)$. By contrast, POLY_n and $\mathcal{Q}_n$ are far richer than CUT_n, and our $K_{m,m} - M$ family exhibits bounded distortion < 1.15 even as $\kappa_{\mathrm{CUT}_{2m}} \to 2$. Does $\kappa_{\mathcal{Q}_n}(G)$ remain $O(1)$ on bounded-degree expanders, or does an $\omega(1)$—perhaps $\Omega(\log n)$—entropic metric distortion barrier survive in $\mathcal{Q}_n$?

References

[1] C. Rajski, *A metric space of discrete probability distributions*, Information and Control **4** (1961), 371–377.

[2] C. H. Bennett, P. Gács, M. Li, P. M. B. Vitányi, and W. H. Zurek, *Information distance*, IEEE Transactions on Information Theory **44** (1998), no. 4, 1407–1423.

[3] Z. Zhang and R. W. Yeung, *On characterization of entropy function via information inequalities*, IEEE Transactions on Information Theory **44** (1998), no. 4, 1440–1452.

[4] N. Linial, E. London, and Y. Rabinovich, *The geometry of graphs and some of its algorithmic applications*, Combinatorica **15** (1995), no. 2, 215–245.

[5] N. Pippenger, *The inequalities of quantum information theory*, IEEE Transactions on Information Theory **49** (2003), no. 4, 773–789.

[6] M. Horodecki, J. Oppenheim, and A. Winter, *Partial quantum information*, Nature **436** (2005), 673–676; also *Quantum state merging and negative information*, Communications in Mathematical Physics **269** (2007), 107–136.

[7] N. Linden and A. Winter, *A new inequality for the von Neumann entropy*, Communications in Mathematical Physics **259** (2005), 129–138.

[8] J. Cadney, N. Linden, and A. Winter, *Infinitely many constrained inequalities for the von Neumann entropy*, IEEE Transactions on Information Theory **58** (2012), no. 6, 3657–3663.

[9] M. Hutter, *Properties of Algorithmic Information Distance*, arXiv:2507.21988 (2025).

[10] F. Hou, *Complete bipartite embeddings, lattice non-embeddability, and non-Euclidean powers of information distance*, arXiv:2609.38919 (2026).

[11] E. H. Lieb and M. B. Ruskai, *Proof of the strong subadditivity of quantum-mechanical entropy*, Journal of Mathematical Physics **14** (1973), 1938–1941.

[12] M. M. Deza and M. Laurent, *Geometry of Cuts and Metrics*, Algorithms and Combinatorics **15**, Springer, 1997.